LAWRENCE
LIVERMORE
NATIONAL
LABORATORY

Crustal thinning between the Ethiopian and East African Plateaus from modeling Rayleigh wave dispersion

M. H. Benoit, A. A. Nyblade, M. E. Pasyanos

January 18, 2006

Disclaimer

This document was prepared as an account of work sponsored by an agency of the United States Government. Neither the United States Government nor the University of California nor any of their employees, makes any warranty, express or implied, or assumes any legal liability or responsibility for the accuracy, completeness, or usefulness of any information, apparatus, product, or process disclosed, or represents that its use would not infringe privately owned rights. Reference herein to any specific commercial product, process, or service by trade name, trademark, manufacturer, or otherwise, does not necessarily constitute or imply its endorsement, recommendation, or favoring by the United States Government or the University of California. The views and opinions of authors expressed herein do not necessarily state or reflect those of the United States Government or the University of California, and shall not be used for advertising or product endorsement purposes.

Crustal thinning between the Ethiopian and East African Plateaus from modeling Rayleigh wave dispersion

Margaret H. Benoit and Andrew A. Nyblade, Department of Geosciences, Penn State University, University Park, PA 16802. mbenoit@geosc.psu.edu
Michael E. Pasyanos, Geophysics and Global Security, Lawrence Livermore National Labratory, Livermore, CA 94551.

Abstract: The East African and Ethiopian Plateaus have long been recognized to be part of a much larger topographic anomaly on the African Plate called the African Superswell. One of the few places within the African Superswell that exhibit elevations of less than 1 km is southeastern Sudan and northern Kenya, an area containing both Mesozoic and Cenozoic rift basins. Crustal structure and uppermost mantle velocities are investigated in this area by modeling Rayleigh wave dispersion. Modeling results indicate an average crustal thickness of 25+/- 5 km, some 10-15 km thinner than the crust beneath the adjacent East African and Ethiopian Plateaus. The low elevations can therefore be readily attributed to an isostatic response from crustal thinning. Low Sn velocities of 4.1 - 4.3 km/s also characterize this region.

1.0 Introduction

The East African and Ethiopian Plateaus have been recognized for over a decade to be part of a much larger topographic anomaly on the African Plate called the African Superswell that includes the southern African Plateau and a bathymetric swell in the southeastern Atlantic Ocean [Nyblade and Robinson, 1994]. One of the few places within the African Superswell that exhibit elevations of less than 1 km is southeastern Sudan and northern Kenya, an area that contains both Mesozoic and Cenozoic rift basins (Figure 1). The region is ~ 500 km wide with average elevations of ~ 500 m (Figure 1). The Mesozoic basins are part of the Central African Rift System that formed during the breakup of Gondwana [Browne et al., 1985; Binks and Fairhead, 1992; Bosworth, 1992] (Figure 1).

Many authors have suggested that the African Superswell is the surface expression of the African Superplume, a broad through-going mantle upwelling beneath southern and eastern Africa, originating from the core-mantle boundary [Ritsema et al., 1999; Lithgow-Bertelloni and Silver, 1998; Gurnis et al., 2000]. If correct, it is difficult to understand why a significant break in topography would exist between the Ethiopian and East African Plateaus, particularly because broad, deep seated thermal anomalies in the upper mantle have been imaged beneath both the East African and Ethiopian Plateaus, consistent with a superplume origin for the superswell [Benoit et al., 2005; Bastow et al., 2005; Ritsema et al., 1998; Weeraratne et al., 2003; Green et al., 1991; Slack and Davis, 1994].

One possible explanation for the low elevations between the Ethiopian and East African Plateaus is that the crust is anomalously thin because of the multiple episodes of rifting (i.e, the lower elevations reflect, isostatically, the thinning). Previous seismic studies of crustal structure in northern Kenya suggest that the crust has indeed been thinned, at least locally [Simiyu and Keller, 1997, Prodehl et al, 1997 and the references therein], but no comprehensive study exists of crustal structure across the entire region of low elevation. Therefore, it remains unknown if the low elevations regionally could be an isostatic response to the crustal thinning or, alternatively, if the low elevations could represent a fundamental change in mantle structure between the Ethiopian and East African Plateaus. In this study, we investigate crustal thickness and upper most mantle velocities between the Ethiopian and East African Plateaus by modeling Rayleigh wave dispersion to determine if the low elevations could have resulted regionally from crustal thinning.

2.0 Surface Wave Inversion

To investigate crustal and upper most mantle structure between the Ethiopian and East African Plateaus, we first generate surface wave group velocity maps by inverting dispersion measurements of fundamental mode Rayleigh waves. The dispersion measurements were made using data from several permanent and temporary broadband seismic stations in eastern Africa, the Arabian Peninsula, the Middle East, and the Seychelles for periods of 10 to 100 s. The temporary stations used include the Saudi Arabian PASSCAL Network [Vernon et al., 1996], the Tanzania Broadband Seismic Experiment [Nyblade et al., 1996], the Ethiopian Broadband Seismic Experiment, and the Kenya Broadband Seismic Experiment [Nyblade and Langston, 2002].

Group velocity measurements were made using the PGplot Surface Wave Multiple Filter Analysis code (PGSWMFA) [Ammon, personal communication 2003] by applying a narrow-band Gaussian filter to vertical component seismograms, and then picking the maximum amplitude at each period. To maximize ray path coverage, dispersion measurements made in this study were combined with previous dispersion measurements from Eurasia and North Africa from Pasyanos et al., [2001] and Pasyanos and Walter, [2002] yielding a total of ~ 50,000 Rayleigh wave measurements. Ray paths for the new dispersion measurements along with the previous measurements for the periods of interest (10 – 60 s) are shown the supplemental material.

Group velocity dispersion measurements were inverted using the method outlined in Pasyanos et al. [2001] to produce maps showing spatial variability in group velocity for periods of 10 to 100 s. The inversion was performed using a 1.5°X 1.5° grid and a

conjugate gradient method, which works well on sparse linear systems. In the inversion, the data were weighted using quality estimates of the dispersion measurements. A smoothing constraint was also applied to the data to control the tradeoff between fitting the data and smoothing the models.

Results of the inversion show substantial lateral velocity heterogeneity. Examples of group velocity dispersion curves produced by the inversion, shown in Figure 2, show regional variability between the different tectonic regions. Maps of the inversion results, found in the supplementary material, also show considerable velocity heterogeneity across the region. The shorter period group velocity maps (10-30 s) reflect shallower crustal structures, such as sedimentary basins, and differentiate between oceanic and continental crust. Longer period surface waves (40-60 s) begin to sample mantle structure. Some deeper features such as the lithospheric keel of the Tanzania craton and the thermally perturbed mantle under the East African Rift system are visible at periods of 50 and 60 s (supplementary material). In southeastern Sudan slower than average velocities can be seen at 10 s period, faster than average velocities from 20 – 40 s period, and slower than average velocities at 50 and 60 s period. At 10 and 20 s periods, group velocities in northern Kenya are faster than average, but slower than average from 30 to 60 s period.

To evaluate the resolution of the group velocity models, we generated synthetic travel times using the same ray paths as our data for different 'checkerboard' models, and then inverted the synthetic dispersion data using the same parameters we used to

invert our data. The results of three checkerboard tests at 20, 40 and 60 s using 4°x 4°

squares are provided in the supplementary material. The checkerboards are well resolved

for each test in continental regions of the model.

3.0 Constrained Grid Search

Next, the surface wave group velocity maps were used with a grid search

technique to create a layered earth model. A grid search method was chosen to do this

because *a priori* information can be easily included in the model search, and because it is

straightforward to see how various tradeoffs in model parameters affect the results.

The model domain for the grid search was parameterized using 1°X 1° blocks and

three layers in depth: a near surface sediment layer, a crustal layer, and an upper mantle

layer. The upper mantle was parameterized as a 30 km thick layer over the ak135 model

[Kennett et al., 1995] to a depth of 150 km. In the grid search, crustal thickness (H) was

allowed to vary between 15-45 km, sediment thickness (S) from 0-6 km, upper mantle S

velocities (Sn) from 4.1-4.6 km/s, and crustal Poisson's ratio (σ_c) from 0.24-0.30. We

assumed that sediment S velocities were 1.9 km/s from the surface to 2 km depth, and

then 2.8 km/s for sediments deeper than 2 km.   The crustal S velocity and the mantle

Poisson's ratio were held constant for each inversion, though several values of each were

tested. We fixed the crust and upper mantle structure in parts of Ethiopia, Tanzania,

Uganda and Kenya where constraints exist from seismic refraction, Pn tomography, and

receiver function studies on the crustal thickness, sediment thickness, Poisson's ratio, and

Pn velocity [Brazier et al., 2000; Last et al., 1997; Dugda et al., 2005; Prodehl et al., 1997

and references therein](Figure 3).

Best fitting models were selected based on a misfit estimation that minimizes the group velocity residual divided by the uncertainty measurements of the group velocity dispersion curve generated from the surface wave velocity maps. The uncertainty measurements from the surface wave maps are estimated by using a bootstrapping method. The misfit equation is:

$$misfit = \sqrt{\left[\sum_{i=1}^{n}\left(\frac{U_m^i - U_d^i}{s_d^i}\right)^2\right] \bigg/ n}$$

where U_m is the group velocity from the model, U_d is the group velocity from the surface wave velocity maps (i.e., the data), s_d is the data uncertainty, and i is the loop over the periods from 1 to n [Pasyanos and Walter, 2002]. A perfect fit to the data would have a misfit of 0, while a model fitting all points at one standard deviation would produce a misfit of 1, providing a scale to assess how well the data is being fit by the models. Using this scale, all of the models with misfit functions < 1 are considered reasonable models with respect to the data uncertainty.

Figures 3 a-d show maps of the model parameters (H, S, Sn, and σ_c) obtained from the grid search. Throughout the region of low elevations between the Ethiopian and East African Plateaus, crustal thickness ranges from 30 to 20 km (Figure 3a), and average sediment thicknesses of 1 km are obtained, with thickness increasing to 3 km along the Kenya coast and in the northwestern portion of the rifted region in Sudan (Figure 3b). Sediment thickness locally within the rift basins probably exceeds these estimates, which represent average structure across the basins as a result of the grid spacing used in the modeling. The Sn velocities range between 4.1 − 4.3 km/s throughout the region of low

elevation (Figure 3c), and crustal Poisson's ratio ranges from 0.26-0.30 with an average of 0.28 (Figure 3d).

To assess the effect of using a single average S wave velocity (set as an *a priori* constraint) for the crust, we ran separate grid searches using S velocities that ranged from 3.52 - 3.71 km/s. The effects on the model parameters are shown in Table 1. While changing the average crustal velocity had little effect on the average Moho depth, average Sn velocities, or average crustal Poisson's ratio, the thickness of the sediment layer increased by ~ 0.25 km for every ~0.3 km/s increase in average crustal velocity. The mantle Poisson's ratio was also varied in separate grid searches from 0.27 to 0.29, but this had little effect on the grid search results.

By examining the rms misfit values associated with the parameters used in the grid search, we can evaluate the uncertainties in each parameter. 1-D slices through the parameter space and the corresponding rms misfit for crustal thickness, Sn velocity, crustal Poisson's ratio, and sediment thickness for southern Sudan and northern Kenya are shown in the supplementary material. In these regions, the uncertainties in crustal thickness are ± 5 km, ± 0.15 km/s for Sn velocity, ± 0.02 for Poisson's ratio, and ±1 km for sediment thickness.

4.0 Discussion

The results of the grid search indicate that the crust is thinned significantly in the region of low elevation between the Ethiopian and East African Plateaus. The average crustal thickness in the plateaus is ~ 38 km, while the average crustal thickness between the plateaus is ~ 25 +/- 5 km. Low Sn velocities (4.1 – 4.3 km/s) also characterize the

region of low elevations. These Sn velocities are comparable to Sn velocities found under the Cenozoic Kenya Rift and Main Ethiopian Rift (Simiyu and Keller, 1997; Prodehl et al., 1997 and references therein; Mackenzie et al., 2005], and indicate that upper most mantle temperatures in this region are elevated.

Using the crustal thickness estimates shown in Figure 3a, we can now investigate whether the low elevations between the Ethiopian and East African Plateaus could result from crustal thinning. Assuming Airy isostasy, we calculate the expected difference in average elevation across the region of thinned crust between the Ethiopian and East African Plateaus. For Airy isostasy, uplift $U = r(\rho_m - \rho_c)/ \rho_c$, where r is the difference in crustal thickness, ρ_m is the mantle density, and ρ_c is the crustal density.   For r ~ 13 km (i.e., 25 km versus 38 km thick crust), ρ_c of 2.8 g/cm^3, and ρ_m of 3.2 g/cm^3, 1.8 km of differential elevation can be accounted for by isostasy. This result is consistent with the observed difference in elevation between the Ethiopian and East African Plateaus and the region of low elevation in between them (Figure 1).

Estimates of crustal thickness shown in Figure 3 are also consistent with gravity models of the region. Bouguer gravity anomalies within the region of low elevation are ~ -60 to 100 mGals [Simiyu and Keller, 1997], at least within the vicinity of the Cenozoic Turkana rift.   An anomaly of this size can be accounted for with a thin crust (~20 km) over a hot (i.e. low density), buoyant mantle [Simiyu and Keller, 1997].

5.0 Conclusions

The results of this study indicate that lower elevations found between the Ethiopian and East African Plateaus likely reflect an isostatic response to crustal

thinning. The crust is thinner than normal across this fairly wide region (~ 500 km),

probably because of the superposition of the multiple phases of rifting in the Mesozoic

and Cenozoic. If the crust in this region had not been thinned by ~ 10 – 15 km, then the

high elevation of the Ethiopian and East African Plateaus would be continuous and these

plateaus would not be seen as geographically distinct regions of uplift. Because the

variations in elevation can be readily attributed to crustal thinning, there is little reason to

suspect fundamental changes in mantle structure between the Ethiopian and East African

Plateaus.

References

Bastow, I.D., G.W. Stuart, J.-M. Kendall, and C.J. Ebinger, Upper mantle seismic

   structure in a region of incipient continental breakup: northern Ethiopian rift, *J.

   Geophys. Res., 162, 479-493*, 2005.

Benoit, M. H., A.A. Nyblade, and J.C. VanDecar, Upper mantle P wave speed variations

   beneath Ethiopia and the origin of the Afar Hotspot, *Geology*, in press, 2005.

Binks, R.M. and J.D. Fairhead,A plate tectonic setting for Mesozoic rfits of west and

   central Africa, *Tectonophysics, 213*, 141-151, 1992.

Bosworth, W., Mesozoic and earth Tertiary rift tectonics in East Africa., in *Seismology

   and Related Sciences in Africa*, edited by C.J. Ebinger, H.K. Gupta, and I.O.

   Nyambok, *Techtonophysics*, 209,115-137, 1992.

Brazier, R.A., A.A. Nyblade, and C.A. Langston, Pn wave velocities beneath the
Tanzania craton and adjacent rifted mobile belts, East Africa, *Geophys. Res. Lett.,
27*, 2365–2368, 2000.

Browne, S.E., J.D. Fairhead, and I.I. Mohammed, Gravity study of the White Nile rift,
Sudan, and its regional setting, *Tectonophysics, 113*, 123-137, 1985.

Dugda, M.T., A.A. Nyblade, J. Julia, C.A. Langston, C.J. Ammon, and S. Simiyu, Crustal
structure in Ethiopia and Kenya from receiver function analysis: Implications for
rift development in eastern Africa, *J. Geophys. Res., 110*, doi:
10/1029/2004JB003065, 2005.

Green, W.V., U. Achauer, and R.P. Meyer, A three-dimensional seismic image of the
crust and upper mantle beneath the Kenya rift, *Nature, 354*, 199-203, 1991.

Gurnis, M., J. X. Mitrovica, J. Ritsema, and H.-J. van-Heijst, Constraining mantle density
structure using geological evidence of surface uplift rates: The case of the African
Superplume, *Geochem. Geophys. Geosyst., 1*, Paper number 1999GC000035,
2000.

Kennett, B.N.L., E.R. Engdahl, and R. Buland, Constraints on seismic velocities in the
Earth from travel times, *Geophys. J. Int, 122*, 108-124, 199

Last, R. J., A.A. Nyblade, C.A. Langston, and T.J. Owens, Crustal structure of the East
African Plateau from receiver functions and Rayleigh wave phase velocities, *J.
Geophys. Res., 102*, 24469-24483, 1997.

Lithgow-Bertelloni, C., and P. G. Silver, Dynamic topography, plate driving forces and
the African Superswell, *Nature, 395*, 269–272, 1998.

Mackenzie, G.D., H. Thybo, and P.K.H. Maguire, Crustal velocity structure across the Main Ethiopian Rift: results from two-dimensional wide-angle seismic modeling, *Geophys. J. Int, 162*, 994-1006, 2005.

Nyblade, A.A., C. Birt, C.A. Langston, T.J. Owens, and R.J. Last, Seismic experiment reveals rifting of craton in Tanzania, *Eos Trans. AGU, 77*, 517, 520-521, 1996.

Nyblade, A.A., and C.A. Langston, Broadband seismic experiments probe the East African Rift, *EOS Trans. AGU, 83*, 405-408, 2002.

Nyblade, A.A., and S.W. Robinson, The African superswell, *Geophys. Res. Lett., 21*, 765-768, 1994.

Pasyanos, M.E. and W. R. Walter, Crust and upper-mantle structure of North Africa, Europe and the Middle East from inversion of surface waves, *Geophys. J. Int., 149*, 463-481, 2002.

Pasyanos, M.E., W.R. Walter, and S.E. Hazler, A surface wave dispersion study of the Middle East and North Africa for monitoring the Comprehensive Nuclear-Test-Ban Treaty, *Pageoph, 158*, 1445-1474, 2001.

Prodehl, C., J.R.R. Ritter, M. Mechie, G.R. Keller, M.A. Khan, B. Jacob, K. Fuchs, I.O. Nyambok, J.D. Obel, and D Riaroh, The KRISP 93/94 lithospheric investigations of southern Kenya - the experiments and their main results, *Tectonophysics, 278*, 121-147, 1997.

Ritsema, J., A. A. Nyblade, T. J. Owens, C. L. Langston, and J. C. VanDecar, Upper mantle seismic velocity structure beneath Tanzania, east Africa: Implications for the stability of cratonic lithosphere, *J. Geophys. Res., 103*, 21,201–21,213, 1998.

Ritsema, J., H. J. van Heijst, and J. H. Woodhouse, Complex shear wave velocity structure beneath Africa and Iceland, *Science, 286,* 1925– 1928, 1999.Slack, P.D. and P.M. Davis, The seismic attenuation and velocity of P wave in the mantle beneath east African rift, Kenya, *Tectonophysics, 236*, 331-358, 1994.

Simiyu, S. M. and G. R. Keller, An integrated analysis of lithospheric structure across the East African Plateau based on gravity anomalies and recent seismic studies, *Tectonophysics, 278*, 291-313, 1997.

Vernon, F., R. Mellors, J. Berger, A. Edelman, A. Al-Amri, J. Zollweg, and C. Wolfe, Observations from regional and teleseismic earthquakes recoreded by a deployment of broadband seismometers in the Saudi Arabian Shield, *Eos Trans. AGU, 77*, 46, 478, 1996.

Weeraratne, D.S., D.W. Forsyth, K.M. Fischer, and A.A. Nyblade, Evidence for an upper mantle plume beneath the Tanzanian craton from Rayleigh wave tomography, J. Geophys. Res., 108(B9), 2427, doi:10.1029/2002JB002273, 2003.

Figure Captions

Figure 1. Map of eastern Africa showing surface elevation and the outline of Mesozoic rifts in Sudan and Kenya (narrow dashed lines) and the Cenozoic East African Rift (bold dashed lines). The Tanzania craton is outlined with a dotted black line, and the Central African Shear Zone (CASZ) is shown as black lines.

Figure 2. Example dispersion curves produced by the inversion for the East African Plateau, the Sudan Rift, the Anza Rift, and the Ethiopian Plateau.

Figure 3. Maps of (a) crustal thickness, (b) sediment thickness, (c) Sn velocity, and (d) crustal Poisson's ratio obtained from the grid search. The areas shown with crosses and outlined by a solid black line denote regions where the grid search was constrained (see text for further explanation).

Figure 4 – supplementary material. a-f) Maps showing ray path coverage for 10 to 60 s period Rayleigh waves. Yellow circles and red triangles represent event locations and station locations, respectively. Blue lines represent ray paths from Pasyanos et al., [2001], and green lines show ray paths added in this study.

Figure 5 - supplemental material.   Maps showing Rayleigh wave group velocity variations for 10 to 60 s periods obtained by inverting dispersion measurements for source-receiver paths shown in Figure 4.

Figure 6 – supplementary material. Maps of recovered velocity models for an input checkerboard pattern at (a) 20 s, (b) 40 s, and (c) 60 s. The political boarders and coastlines are outlined in solid white, and the checkerboard squares are 4° x 4°.

Figure 7 – supplementary material. Graphs showing rms misfit values obtained from the grid search for (a) crustal thickness, (b) Sn velocity (c) Poisson's ratio and (d) sediment thickness for 7°N, 32°E (southern Sudan).

Figure 8 – supplementary material. Graphs showing rms misfit values obtained from the grid search for (a) crustal thickness, (b) Sn velocity (c) Poisson's ratio and (d) sediment thickness for 3°N, 38°E (northern Kenya).
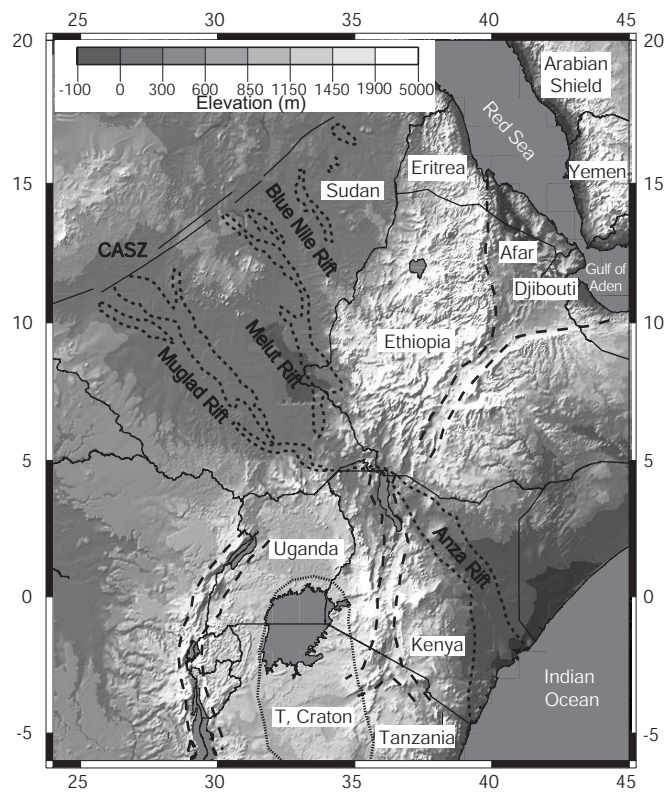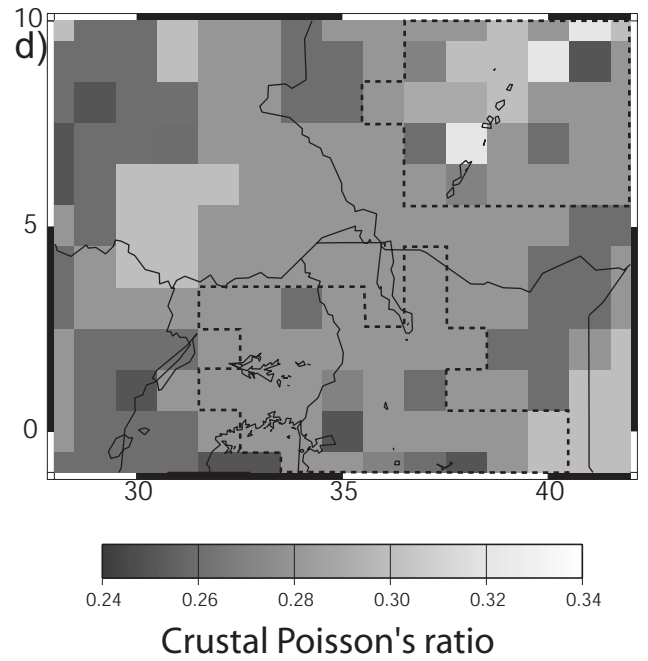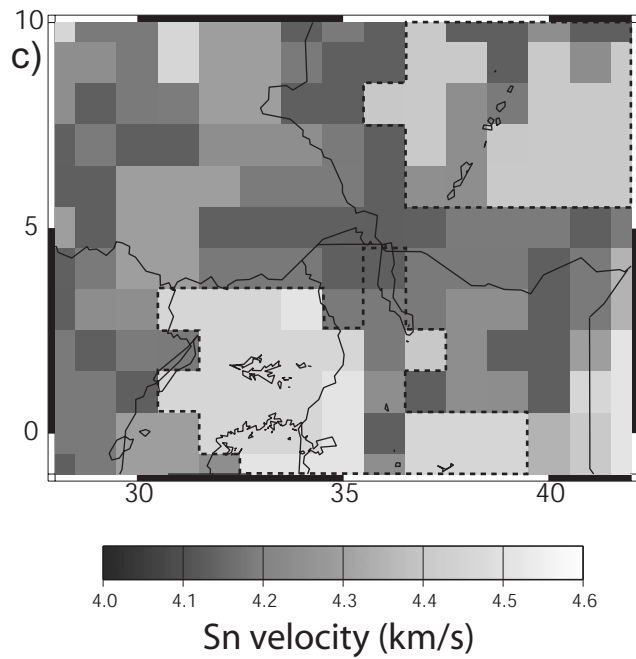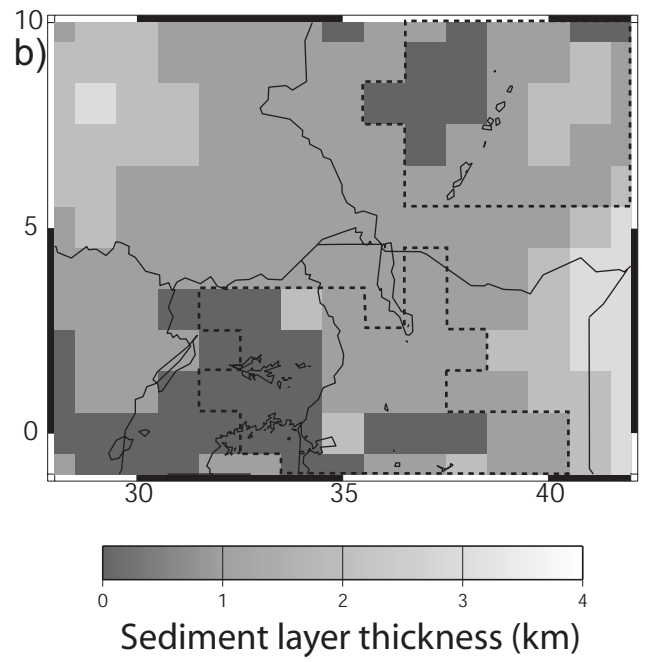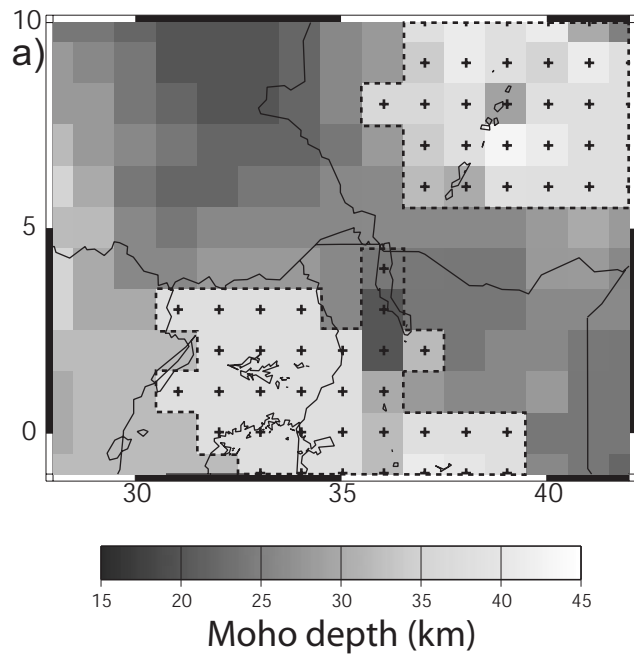
Benoit et al., Figure 1
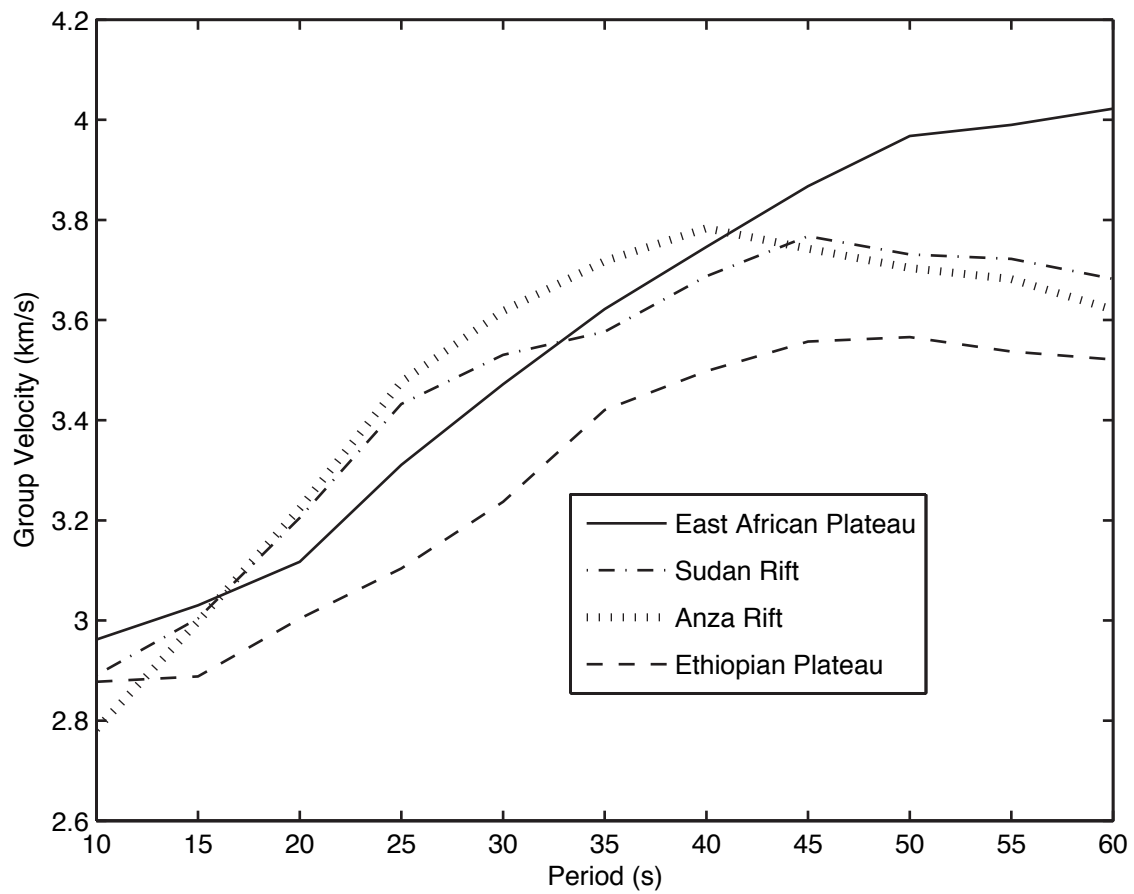
Benoit et al., Figure 2

Table 1: Table showing the effects on the model parameters when the average crustal velocity and average mantle Poisson's ratio are held constant for each grid search.

Average crustal Vs (km/s)	Average mantle σ	Average sediment thickness (km)	Average crustal thickness (km)	Average Sn velocity (km/s)	Average crustal σ
3.55	0.29	1.19	26.70	4.17	0.267
3.58	0.29	1.33	27.26	4.18	0.271
3.63	0.29	1.61	28.26	4.19	0.272
3.69	0.29	1.97	29.56	4.20	0.272
3.71	0.29	2.26	30.00	4.35	0.278
3.52	0.27	0.99	26.49	4.27	0.272
3.52	0.28	1.09	26.30	4.20	0.272

Benoit et al., Figure 3